Spatial Node Distribution of the Random Waypoint Mobility Model with Applications

Esa Hyytiä[†], Pasi Lassila, and Jorma Virtamo, *Member, IEEE*

Networking Laboratory, Helsinki University of Technology,
P.O. Box 3000, FIN 02015 TKK, Finland

Email: Esa.Hyytia@iki.fi, {Pasi.Lassila, Jorma.Virtamo}@tkk.fi

Abstract— The random waypoint model (RWP) is one of the most widely used mobility models in performance analysis of ad hoc networks. We analyze the stationary spatial distribution of a node moving according to the RWP model in a given convex area. For this we give an explicit expression, which is in the form of a one-dimensional integral giving the density up to a normalization constant. This result is also generalized to the case where the waypoints have a non-uniform distribution. As a special case, we study a modified RWP model, where the waypoints are on the perimeter. The analytical results are illustrated through numerical examples. Moreover, the analytical results are applied to study certain performance aspects of ad hoc networks, namely connectivity and traffic load distribution.

Index Terms— mobility modeling, random waypoint model, ad hoc networking, connectivity

I. INTRODUCTION

Analysis of wireless systems, either via simulation or analytical modeling, often requires that the effect of node (or user) mobility on system performance can be modelled. The construction and use of mobility models based on the actual, say, measured characteristics of mobile nodes is difficult. Instead, one often uses elementary synthetic mobility models, which still capture the essential impact of mobility on the performance measure under study. The advantage of using synthetic models is that they can be more easily treated in analysis or implemented in simulations.

The most widely used synthetic mobility model is the Random Waypoint model (RWP), which was originally proposed for studying the performance of ad hoc routing protocols by Johnson and Maltz [1]. In this model, a mobile node moves in a convex domain along a zigzag path, where each of the straight line segments is called *a leg*. At each turning point the node chooses a new destination randomly and then moves towards the destination at a constant speed, which is drawn independently from a given speed distribution at each turning point. The node may also remain stationary for a random pause time before starting its movement towards the next destination.

Analytical performance evaluation of ad hoc networks requires analyzing the properties of the mobility models. For example, one important intrinsic property of any mobility model

is the distribution of the node location (or shortly the node distribution), which may be far from uniform. On the other hand, the uniform distribution is commonly assumed in many performance studies, for example in studies on ad hoc network capacity (see, e.g., [2] and [3]) and connectivity properties of random networks (see, e.g., [4], [5], and [6]). Thus, knowledge of the actual node distribution is often needed in order to study the impact of mobility on the performance measure of interest.

In this paper, we derive an explicit expression for the node distribution of RWP in an arbitrary convex domain and demonstrate the use of the result for various shapes of the domain. Accurate polynomial approximations for the density function are derived for a regular triangle, square and hexagon. We comment on the relation of our results to other related work separately in Section I-A. Additionally, a generalized RWP model is considered, where the waypoints may have an arbitrary distribution, for which a general expression for the node distribution is derived. As a special case of this, we further study a variant of the RWP model, named as RWPB, where the waypoints are located on the perimeter of the area. The motivation for introducing and analyzing the RWPB model is that, whereas the RWP model yields a distribution that concentrates more probability mass near the center of the domain, the RWPB model gives a distribution with more probability mass near the edges than in the center. Hence, these models serve as two elementary mobility models with fundamentally different spatial characteristics, and any practical networking mechanism should be robust with respect to different mobility patterns. As an application of our results, we consider the connectivity properties of ad hoc networks. In particular, we compare the impact of nodes moving according to either RWP or RWPB against the assumption of nodes being uniformly distributed in the area. Knowledge of the exact node distribution allows the derivation of accurate polynomial approximations. Such approximations facilitate numerical computations in another application, where we study the impact of node mobility on the traffic load distribution in ad hoc networks with shortest path routing.

The rest of the paper is organized as follows. Section II introduces the traditional RWP model together with some of the notation. The RWP model is analyzed in Section III, where analytic expressions for the node distribution and its polynomial approximations are derived and illustrated for

† Currently working at the Centre for Quantifiable Quality of Service in Communication Systems, Centre of Excellence, Norwegian University of Science and Technology, O.S. Bragstads plass 2E, N-7491 Trondheim, Norway.

several geometries. Correspondingly, the results for the generalized RWP model with an arbitrary waypoint distribution are given in Section IV. Applications of our results are given in Section V. Section VI contains our conclusions.

A. Related work and our contribution

The RWP model and its spatial properties have been analyzed recently in a number of other papers. The observation that the initial definition of the speed distribution (i.e., the uniform distribution in the range $[0, v_{\max}]$) was indeed ill-defined was made in [7]. Since then the same observations have been made in several other papers as well, see, for example [8], [9] and [10]. The impact of the speed distribution on simulations is further discussed in [11] for more general mobility models.

Concerning the derivation of the node distribution, results for some special shapes of the movement region have been given in [8], [9], [12], and [13]. Navidi and Camp [8] basically give the definition of the node distribution in a rectangular area, resulting in a four-dimensional integral over all possible locations of the starting and ending points. Using our approach, we are able to simplify this expression considerably (in an arbitrary convex domain). In [12] and [13], Bettstetter et al. derive simple explicit results for the node distribution in circular and rectangular regions ([9] contains new results on temporal properties of RWP and repeats the results on the node distribution from [13]), but the derivations have been performed using approximations at certain steps resulting in slight inaccuracy in the results (as indicated in our numerical examples).

Our analysis is similar to that of Bettstetter et al. in [13]. However, we complete the analysis without using approximations or a special shape for the region and derive an explicit analytical expression for the node distribution in an arbitrary convex region. The point at which our analysis differs from [13] is indicated in our derivation in Section III. As mentioned earlier, the direct application of the definition for the node distribution results in a four-dimensional integral. We are able to simplify the expression to a one-dimensional integral, which gives the distribution up to a normalization constant. The evaluation of the normalization constant requires integration of the density expression over the considered region. Our result was first given in report form in [14]. A generalization of this result to $\mathbb{R}^n$ has been published in [15].

We also give results on the mean length of a leg, which can be obtained in our case in two ways. The mean length of a leg can be related to the normalization constant. On the other hand, it can be expressed as a four-dimensional integral, which we reduce to a two-dimensional one (in Appendix). Note that the results for the mean leg length can be also found in the literature (see, e.g., "line picking" problems in [16], [17] and [18]).

More recently, independent of our work, the theory of Palm calculus has been applied for analyzing RWP in [10] and [19]. The main result in [19] is that the stationary node distribution is independent of the velocity distribution. This issue is also discussed in [7], [11] and [9], and we take this property

established. In [10], a much more general class of mobility models, of which RWP is a special case, is treated formally using Palm calculus. The paper discusses both transient and time stationary distributions of these processes, and the aim is to develop simulation methods, where the process can be initialized according to the stationary state of the system, thus avoiding any special transient handling. However, the formal results on the distributions cannot be readily applied for obtaining explicit expressions of the node distribution, e.g., for RWP that can be numerically evaluated easily.

Also, we note that the properties of the RWP process are in some sense related to the theory of Poisson line processes studied in the field of stochastic geometry, see, e.g., [20]. Typically the processes in stochastic geometry are treated on an infinite plane, but in RWP the region of motion is bounded. To the best of our knowledge, results as explicit as ours are not available from this field of science either.

We additionally derive the node distribution for the RWP model in $\mathbb{R}^2$ with the generalization that the waypoint distribution can be arbitrary (instead of the uniform distribution). As a special case of that, we consider a modified RWP process introduced in [12], where the waypoints are always on the perimeter of the region. As mentioned earlier, this model, referred to as the RWP on border (RWPB), has a node distribution fundamentally different from the node distribution of RWP. The RWPB model has been analyzed using simulations in [12]. Again, the model fits in the framework as studied in [10], but to utilize the results requires Palm calculus. We derive our result using the same method as for RWP giving a simple explicit numerically integrable expression for the node distribution.

An application of the analysis presented in this paper is the use of the results for the derivation of more efficient simulation methods. Yoon et al. [11] have illustrated how, for a class of mobility models, the transient time can be substantially shortened by sampling the initial node speed from the known stationary node speed distribution. However, in a simulation of any mobility model, just initializing the speed appropriately still leaves the transient corresponding to the time until the node location obeys its stationary distribution. For the RWP model, Navidi and Camp [8] have utilized their theoretical results for deriving algorithms with which the entire state (speed and location) of the RWP model (with and without pause times) can be initialized according to its stationary state. Le Boudec and Vojnović [10] refer to this way of initialization as perfect simulation, and they show how this can be achieved for a large class of simulation models by applying the insights from using Palm calculus. Our results can be used to facilitate the generation of samples from the stationary node distribution, and we comment on this briefly later on.

As an application of our results with impact on ad hoc networking, we consider connectivity properties of ad hoc networks. More specifically, we concentrate on the probability that a given network of n nodes, each moving according to RWP (or RWPB), is connected. As a part of our earlier work in [21], we have derived a very accurate approximation for connectivity under the assumption of nodes moving according
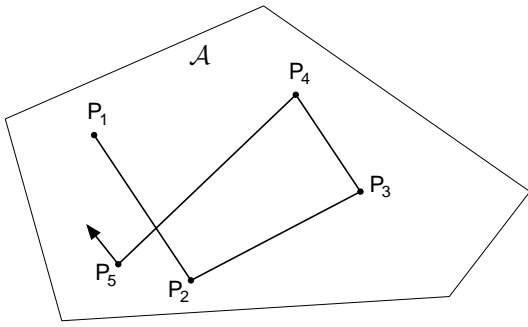
Fig. 1. Zigzag movement of the RWP process.

to the RWP model. However, in this paper we use those results to compare connectivity properties of RWP and RWPB. Our approach to approximate the connectivity is similar to the one in [22], with the distinction that our results have been obtained using exact results for the node distribution. Finally, both our approximation and the one used in [22] are motivated by the theoretical results found in [5] and [23].

Another networking application of our analytical results concerns evaluating the traffic load distribution in ad hoc networks. An analytical model for this has been given in [24] and [25], where it has been assumed that the node distribution obeys a uniform distribution. We study how nodes moving according to the RWP model affect the traffic load distribution using a similar approach as in [24] and [25].

II. RANDOM WAYPOINT MOBILITY MODEL

The process representing the movement of a node within a convex area $\mathcal{A} \subset \mathbb{R}^2$ according to the RWP model can be described as follows. Initially, the node is placed at the point P_1 chosen from a uniform distribution over $\mathcal{A}$. Then a destination point (also called waypoint) P_2 is chosen from a uniform distribution over $\mathcal{A}$ and the node moves along a straight line from P_1 to P_2 with constant velocity V_1 drawn independently of the location from a velocity distribution with pdf $f_V(v)$. Once the node reaches P_2, a new destination point, P_3, is drawn independently from a uniform distribution over $\mathcal{A}$ and velocity V_2 is drawn from $f_V(v)$ independently of the location and V_1. The node again moves at constant velocity V_2 to the point P_3, and the process repeats. Formally, the RWP process is defined as an infinite sequence of triples [9],

$$(P_0, P_1, V_1), \ (P_1, P_2, V_2), \ (P_2, P_3, V_3), \ \ldots \quad (1)$$

This is illustrated in Fig. 1. Thus, the path of a node consists of straight line segments, called legs, defined by a sequence of independently and uniformly distributed waypoints, $\{P_i\}$, in a convex set $\mathcal{A} \subset \mathbb{R}^2$. Furthermore, on each leg (P_{i-1}, P_i) the node velocity V_i is an i.i.d. random variable independent of the node location having the pdf $f_V(v)$. It is also possible to extend the model by defining random pause times (i.i.d. random variables) at the waypoints. The influence of this generalization on the node distribution can be analyzed in a rather straight forward manner as the process consists of two independent and alternating modes, mobile and stagnant [9].

Next we introduce some notation used throughout our analysis of RWP. Let the random variable $\mathbf{X}$ denote the location of a waypoint P. The waypoints are uniformly and independently distributed over $\mathcal{A}$, i.e., the probability density function (pdf) of $\mathbf{X}$ is

$$g(\mathbf{r}) = \begin{cases} \dfrac{1}{A}, & \mathbf{r} \in \mathcal{A}, \\ 0, & \text{otherwise}, \end{cases}$$

where A denotes the area of the set $\mathcal{A} \subset \mathbb{R}^2$. We denote this uniform distribution by $\mathrm{U}(\mathcal{A})$ and write $\mathbf{X} \sim \mathrm{U}(\mathcal{A})$. The random variable representing the location of the node at an arbitrary point of time is denoted by $\mathbf{R}$ and its pdf by $f(\mathbf{r})$.

Note that two consecutive legs in the RWP process (see (1)) share a common waypoint and thus are not independent. However, many properties of the RWP process can be analyzed by studying the corresponding independent leg process, where the legs are, as the name suggests, independent and identically distributed. Formally, for a given RWP process the corresponding independent leg process can be obtained by considering, e.g., every second leg (see [9] and [13])

$$(P_0, P_1, V_1), \ (P_2, P_3, V_3), \ (P_4, P_5, V_5), \ \ldots \quad (2)$$

For example the stationary node distributions of both processes are the same.

In [1], the velocities were taken from a uniform distribution in the range $[v_{\min}, v_{\max}]$, but any distribution can be used (e.g., the beta distribution and a discrete distribution have been used in [9]). Given the pdf $f_V(v)$ from which the velocities at the waypoints are drawn, the stationary distribution of the velocity for a node moving according to the RWP model is given by $(1/v)f_V(v)$ up to a normalization constant. This is because the time spent on a leg is proportional to $1/v$, and V and $\mathbf{X}$ are independent. From this it is also obvious that for $f_V(v) = \mathrm{U}[v_{\min}, v_{\max}]$ the stationary distribution is only defined for $v_{\min} > 0$. Hence, letting $v_{\min} = 0$ implies that stationarity is never reached or, more precisely, in the stationary state all the nodes are stopped, as pointed out by Yoon et al. in [7] and later by others in [8] and [9]. Finally, note that the stationary distribution of the location of a node and the stationary node velocity distribution are independent of each other, as has been formally shown in [19].

III. SPATIAL NODE DISTRIBUTION WITH ARBITRARY WAYPOINTS

In this section the traditional RWP model is considered. General expressions for the node distribution and the mean length of a leg are derived. The results are then illustrated for the RWP process in some regular geometries, for which also accurate polynomial approximations are derived.

A. Approach and derivation

Consider a convex area $\mathcal{A}$ and a node moving within this area at a speed V according to the RWP from waypoint P_1 at $\mathbf{r}_1$ to waypoint P_2 at $\mathbf{r}_2$. Our aim is to derive the probability density $f(\mathbf{r})$ giving the probability per unit area of finding the node at $\mathbf{r}$.
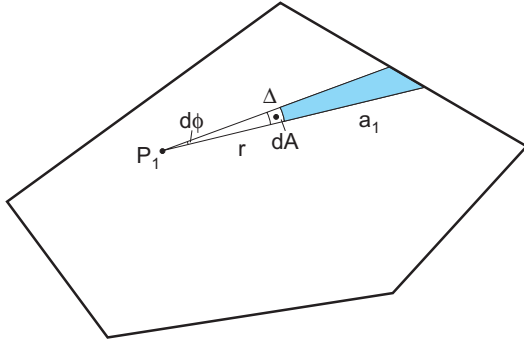
Fig. 2. Illustration of the variables $P_1, d\phi, r, \Delta, dA$ and a_1 (adapted from [13]).

Similarly as in [13], we consider a small area element dA located at $\mathbf{r}$. Let P_1 and P_2 be two consecutive points on the path. Denote by ℓ the length of leg $\overline{P_1 P_2}$, $\ell = |\overline{P_1 P_2}|$, and by $\ell \cap dA$ the length of the leg inside a small area element dA. The desired probability density is the expected proportion of time spent in dA, divided by dA (probability per unit area),

$$f(\mathbf{r}) = \frac{\mathrm{E}[(\ell \cap dA)/V]}{\mathrm{E}[\ell/V] \cdot dA} = \frac{1}{\mathrm{E}[\ell]} \frac{\mathrm{E}[\ell \cap dA]}{dA},$$

i.e., as the speed on each leg is drawn independently of the waypoints, the probability density equals the ratio of expected length of the leg segment inside dA to the mean leg length $\mathrm{E}[\ell]$. The expectation in the numerator is calculated by conditioning on the position $\mathbf{r}_1$ of the point P_1,

$$\mathrm{E}[\ell \cap dA] = \frac{1}{A} \int_{\mathcal{A}} \mathrm{E}\left[\ell \cap dA \,|\, P_1 = \mathbf{r}_1\right] d^2\mathbf{r}_1.$$

The conditional expectation (expectation over all possible locations of P_2) is written as

$$\mathrm{E}\left[\ell \cap dA \,|\, \mathbf{r}_1\right] = \frac{1}{A} \int_{\mathcal{A}} (\ell(\mathbf{r}_1, \mathbf{r}_2) \cap dA) \, d^2\mathbf{r}_2,$$

where we have made it explicit that the line segment ℓ is from $\mathbf{r}_1$ to $\mathbf{r}_2$. We note that these equations are already given in [13], where the authors use an approximation for $\mathrm{E}[\ell \cap dA | \mathbf{r}_1]$. However, no approximation is necessary at this point.

Now refer to Fig. 2, and where the shape of the area dA has been chosen in a special way to facilitate the derivation. (It is easy to see that the result is the same irrespective of the shape of dA.) The intersection of $\ell(\mathbf{r}_1, \mathbf{r}_2)$ and dA is Δ when $\mathbf{r}_2$ is in the shaded area and 0 otherwise. So the integral equals Δ times the shaded area and we have with the notation of the figure,

$$\mathrm{E}\left[\ell \cap dA | \mathbf{r}_1\right] = \frac{1}{A} \Delta \frac{1}{2} d\phi \left((r + a_1)^2 - r^2\right)$$
$$= \frac{dA}{2\,A\,r}(2\,r\,a_1 + a_1^2),$$

since $dA = \Delta\,r\,d\phi$. Substitution into the original definition gives,
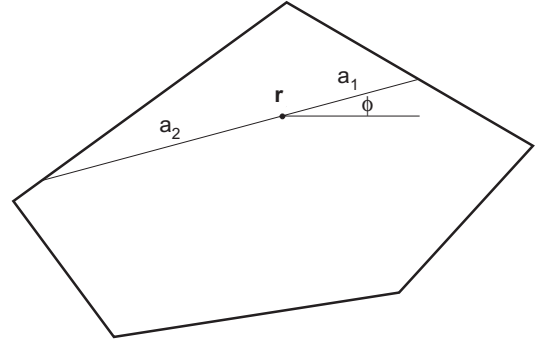
Fig. 3. Illustration of the integral over $[0, 2\pi]$ in (3).

$$f(\mathbf{r}) = \frac{1}{\mathrm{E}[\ell]A^2} \int_{\mathcal{A}} \frac{2\,r\,a_1 + a_1^2}{2\,r} d^2\mathbf{r}_1$$
$$= \frac{1}{\mathrm{E}[\ell]A^2} \int_0^{2\pi} d\phi \int_0^{a_2} \left(r\,a_1 + \frac{1}{2}a_1^2\right) dr,$$

where, in the second form, polar coordinates have been used, $d^2\mathbf{r}_1 = r\,dr\,d\phi$, and a_2 denotes the distance to the boundary in the opposite direction, $\phi + \pi$, as shown in Fig. 3. The radial integral can be evaluated explicitly, yielding the final result

$$f(\mathbf{r}) = \frac{1}{\mathrm{E}[\ell]A^2} \int_0^{2\pi} \frac{1}{2} a_1 a_2 (a_1 + a_2) \, d\phi$$
$$= \frac{1}{\mathrm{E}[\ell]A^2} \int_0^{\pi} a_1 a_2 (a_1 + a_2) \, d\phi, \tag{3}$$

where both a_1 and a_2 are functions of $\mathbf{r}$ and ϕ, $a_1 = a_1(\mathbf{r}, \phi)$ and $a_2 = a_2(\mathbf{r}, \phi)$. The latter form follows because $a_2(\mathbf{r}, \phi) = a_1(\mathbf{r}, \phi + \pi)$, i.e., adding π to ϕ interchanges the roles of a_1 and a_2. The integration turns "the propeller" one turn around, see Fig. 3. For future purposes, we denote the latter integral in (3) by $h(\mathbf{r})$,

$$h(\mathbf{r}) = \int_0^{\pi} a_1 a_2 (a_1 + a_2) \, d\phi. \tag{4}$$

Because $f(\mathbf{r})$ is a distribution integrating to unity, $\int_{\mathcal{A}} f(\mathbf{r}) \, d^2\mathbf{r} = 1$, we immediately obtain

$$\mathrm{E}[\ell] = \frac{1}{A^2} \int_{\mathcal{A}} h(\mathbf{r}) \, d^2\mathbf{r}. \tag{5}$$

An alternative expression for $\mathrm{E}[\ell]$ is given in Appendix A.

B. Example: unit disk

We calculate the node distribution in a unit disk with $A = \pi$. Because of the symmetry the density is a function of the distance $r = |\mathbf{r}|$ only and we write with slight abuse of notation $f(\mathbf{r}) = f(r)$. We can take any point $\mathbf{r}$ with $|\mathbf{r}| = r$; in particular we choose $\mathbf{r} = (0, r)$. Then we see from Fig. 4 that

$$a_1(r, \phi) = \sqrt{1 - r^2 \cos^2 \phi} - r \sin \phi,$$
$$a_2(r, \phi) = \sqrt{1 - r^2 \cos^2 \phi} + r \sin \phi.$$
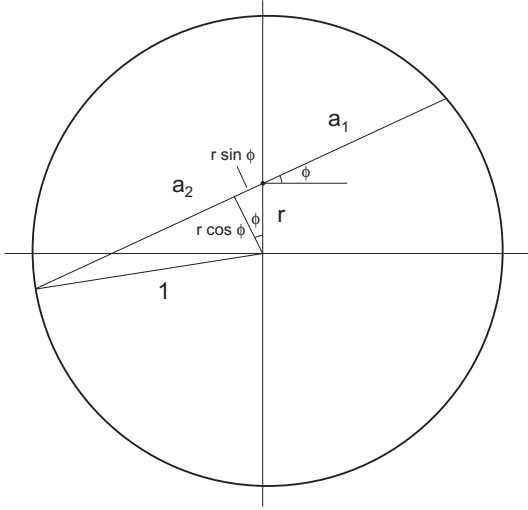
Fig. 4. Derivation of a_1 and a_2 in a unit disk.

Fig. 6. Illustration of the regular triangle, square and hexagon, and the respective symmetric areas.

TABLE II

NORMALIZATION CONSTANT FOR RWP MODEL IN REGULAR POLYGONS.

no. of edges	$n = 3$, triangle	$n = 4$, square	$n = 6$, hexagon
$\mathrm{E}[\ell]$	1.26368	1.04281	0.954082
C	34.1193	16.685	11.449

Thus, $a_1 a_2 = 1 - r^2$ and $(a_1 + a_2) = 2\sqrt{1 - r^2 \cos^2 \phi}$, whence

$$h(r) = 2(1 - r^2) \int_0^\pi \sqrt{1 - r^2 \cos^2 \phi} \, d\phi. \qquad (6)$$

This is an elliptic integral of the second kind and cannot be expressed in terms of elementary functions. However, one can evaluate the normalization constant in a closed form,

$$C = \int_{\mathcal{A}} h(\mathbf{r}) \, d^2\mathbf{r} = 2\pi \int_0^1 r \, h(r) \, dr = \frac{128\,\pi}{45} = 8.936.$$

Thus, the pdf of the node location $\mathbf{r}$ is simply

$$f(r) = \frac{h(r)}{C} = \frac{45(1 - r^2)}{64\,\pi} \int_0^\pi \sqrt{1 - r^2 \cos^2 \phi} \, d\phi. \qquad (7)$$

Then we have the average length of a leg from (3),

$$\mathrm{E}[\ell] = \frac{C}{\pi^2} = \frac{128}{45\pi} \approx 0.905, \qquad (8)$$

in agreement with [16].

In Fig. 5, $f(r)$ is depicted as a function of r along with the probability density function, $f_R(r) = 2\pi r \, h(r)/C$, of the random variable $R = |\mathbf{r}|$. For comparison, the approximation for the node distribution from [12] is illustrated in the same figure with dashed curves (see Table I).

C. Example: polynomial approximation for unit disk

Evaluation of the exact pdf requires numerical integration, which can be too time consuming, e.g., in simulations. For example, when using the rejection method one chooses a point (x, y) uniformly from a unit disk and accepts it with a probability of $f(\sqrt{x^2 + y^2})$. With this in mind one can consider approximating the exact pdf by polynomials of the form

$$P(r) = \frac{(1 - r^2) \cdot (\sum_i a_i r^{2i})}{2\pi \cdot C},$$

where a_i's and B are some (relatively) small integers. As a goodness of fit criterion we use the mean square error,

$$\mathrm{MSE} = \frac{1}{A} \int_{\mathcal{A}} (f(\mathbf{r}) - P(\mathbf{r}))^2 \, d^2\mathbf{r}. \qquad (9)$$

Some reasonably good polynomials of this form are listed in Table I.

D. Example: polynomial approximations for regular polygons

First, we note that it is straightforward to evaluate (3) numerically for any convex polygon. Here our aim is to derive reasonably accurate polynomial approximations for the exact pdf of the node location in the regular polygons illustrated in Fig. 6. The center of each polygon is chosen so that the polygon is symmetrical relative to the x-axis (and possibly to the y-axis also) and the distance from the center to the base is equal to 1. Table II contains the numerical values for the mean leg length $\mathrm{E}[\ell]$ and the normalization constant C for regular triangle, square and hexagon.

Polynomial approximations can be motivated by different reasons. For one, they can be used to generate efficiently samples from the stationary node distribution by using the rejection method. The speed improvement over the existing algorithms (see, e.g., [8] and [10]) is roughly by a factor of two. Secondly, computation of performance quantities based on the stationary node distribution requires integration over all locations, which can be a rather tedious task if the integrand itself is an integral expression. A similar application for polynomial approximations with non-zero even coefficients is discussed later in Section V-B.

To clarify our approach let us first consider a square having corner points at $(-1, -1)$, $(1, -1)$, $(1, 1)$ and $(-1, 1)$. As already mentioned, by choosing the corner points this way the resulting pdf is symmetric relative to both axes and diagonals. It turns out that polynomials of the form

$$\sum_{i,j} a_{ij} (x^2 + y^2)^i (x^2 y^2)^j,$$

exhibit this symmetry. Furthermore, we know that the pdf is zero at the border of the domain and hence the respective lines,

$$x \pm 1 = 0 \text{ and } y \pm 1 = 0,$$
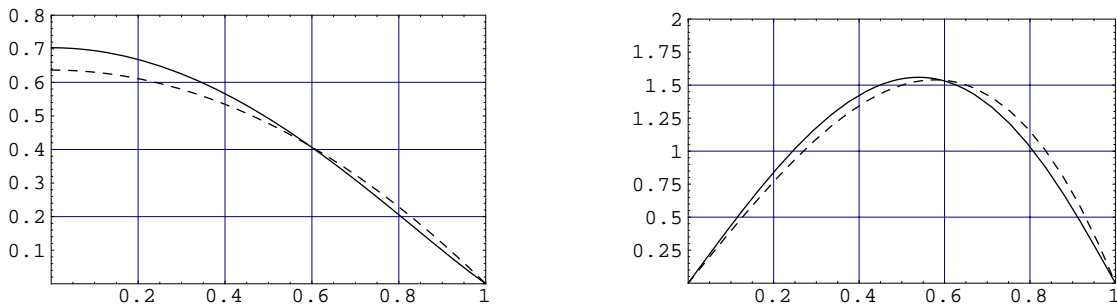
Fig. 5.   The pdf of the node location, $f(r)$, (left) and the pdf of the distance of a node from the origin, $f_R(r)$, (right) for a unit disk. The solid curves correspond to our exact results and the dashed curves to approximation $P_1(r)$ (see Table I).

TABLE I

POLYNOMIAL APPROXIMATIONS OF THE SPATIAL RWP NODE DISTRIBUTION IN UNIT DISK.

degree	polynomial	MSE	max. absolute error
$n=2$	$P_1(r) = \dfrac{2}{\pi}\left(1 - r^2\right)$	$6.5 \cdot 10^{-4}$	0.067 (from [12])
$n=4$	$P_2(r) = \dfrac{6(1 - r^2)(27 - 8r^2)}{73\pi}$	$3.1 \cdot 10^{-6}$	0.0033
$n=6$	$P_3(r) = \dfrac{3(1 - r^2)(189 - 44r^2 - 18r^4)}{257\pi}$	$1.3 \cdot 10^{-7}$	0.00086

should be factors in the polynomial approximation. The symmetry and the boundary requirements lead us to consider polynomials of the form

$$P_4(x,y) = (1 - x^2)(1 - y^2)\sum_{i,j} a_{ij}(x^2 + y^2)^i (xy)^{2j}.$$

Similarly, for (regular) triangle and hexagon the suitable polynomials must be even functions of x and invariant under rotations by $120°$ and $60°$ for triangle and hexagon, respectively. Hence,

$$P_3(x,y) = (1 + y)((2 - y)^2 - 3x^2) \cdot$$
$$\sum_{i,j} a_{ij}(x^2 + y^2)^i (y(3x^2 - y^2))^j,$$
$$P_6(x,y) = (1 - y^2)((y + 2)^2 - 3x^2)((y - 2)^2 - 3x^2) \cdot$$
$$\sum_{i,j} a_{ij}(x^2 + y^2)^i (y(3x^2 - y^2))^{2j}.$$

First we fix the degree of the polynomial, i.e., decide on a finite set of coefficients a_{ij} to be determined. As a fitting criterion we use the mean square error (MSE) given by (9). To ease the computational burden we exploit the symmetry and evaluate the MSE integral only over the shadowed areas in Fig. 6. Table III contains the numerically obtained coefficients. In all cases the obtained polynomial approximation differs from the exact pdf mainly near the corners, where the maximum absolute error is in the range of $0.01 - 0.02$. Fig. 7 illustrates the results for the regular triangle. The fitted polynomial consists of 5 terms resulting in a polynomial of the 8th degree. The MSE is about 0.004, and the maximum absolute error is about 0.014.

For the square we have chosen to fit a polynomial of the 6th degree. The resulting approximation has a MSE of about $1.4 \cdot 10^{-3}$ and a maximum absolute error of about 0.010

which is obtained near the corners. In [13] Bettstetter et al. give an approximation, which is almost as accurate as ours. It turns out that their approximation has a MSE of about $7.1 \cdot 10^{-3}$ and a maximum absolute error of about 0.012, which is obtained in the middle of the region. However, the approximation proposed in [13] has two deficiencies. Firstly, it is defined piecewise in eight symmetrical areas and is not completely smooth across the borders of those areas. Secondly, the expression is rather complex when compared to our polynomial. Fig. 8 illustrates the exact pdf (solid line), our polynomial approximation (dotted line) and the approximation by Bettstetter et al. (dashed line). Note that, the spatial pdf of the node location, e.g., in an arbitrary rectangle with sides a and b, cannot be obtained by simple scaling of the pdf of a square. Hence, if one is considering an arbitrary rectangle, one should evaluate (3) using appropriate expressions for a_1 (and a_2).

Finally, Fig. 9 contains the results for a regular hexagon area. The resulting pdf is already rather close to the pdf in a unit disk. The fitted polynomial was chosen to consist of terms up to the 9th degree, which yields a satisfactory approximation with a MSE of about 0.0012 and a maximum absolute error of about 0.016.

IV. SPATIAL NODE DISTRIBUTION WITH ARBITRARY WAYPOINTS

In this section, we first analyze the RWP model with an arbitrary waypoint distribution. As a special case of this we study a modified RWP model, where the waypoints are always on the perimeter. For this model, we also provide explicit results for the unit disk area and the unit square area.

TABLE III

COEFFICIENTS FOR THE POLYNOMIAL APPROXIMATIONS OF THE NODE DISTRIBUTION IN REGULAR POLYGONS.

case						
$n = 3$	$a_{00} = 0.0904092,$	$a_{10} = 0.0131599,$	$a_{01} = 0.00944523,$	$a_{20} = 0.0209075,$	$a_{11} = 0.000570773$	
$n = 4$	$a_{00} = 0.551066,$	$a_{10} = -0.133986,$	$a_{01} = 1.20532,$	$a_{20} = 0.172301,$	$a_{11} = -1.48645,$	$a_{02} = 3.32898$
$n = 6$	$a_{00} = 0.039526,$	$a_{10} = 0.0193813,$	$a_{20} = -0.0159052,$	$a_{30} = 0.0406354,$	$a_{01} = -0.0236053$	
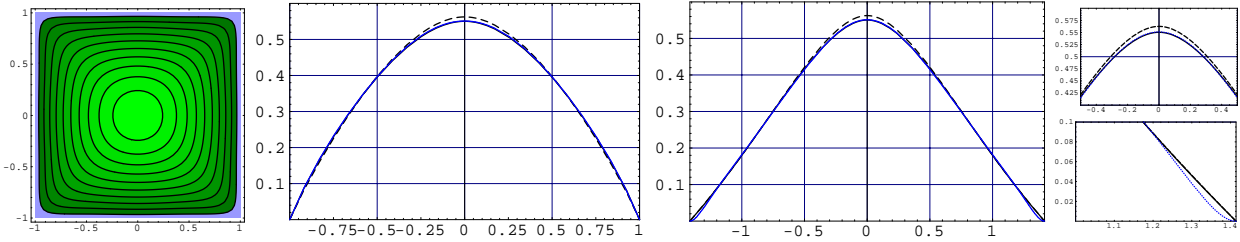
Fig. 8. Equivalue contours and cross sections of the node distribution in a regular square. The middle figure corresponds to the cross section along the x- or y-axis and the right figure corresponds to the cross section along the diagonal. The dashed line corresponds to the approximation given in [13], the dotted line to our polynomial approximation and the solid line to the exact result. The small right-most figures correspond to zoomed areas of the diagonal cross section.
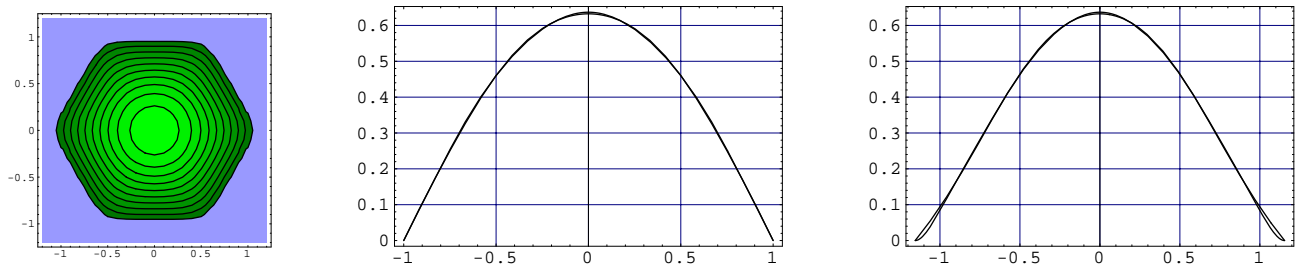
Fig. 9. Equivalue contours and cross sections of the node's location pdf in a hexagonal area. The middle figure corresponds to the cross section along the y-axis and the right figure to the cross section along the x-axis. The difference between the exact pdf and the approximation is very small.
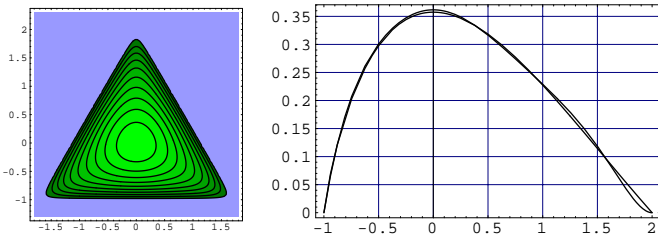
Fig. 7. Equivalue contours, and the exact and approximate pdf in the cross section along the y-axis for a regular triangle ($n = 3$).

A. Approach and derivation

The traditional RWP model is based on the assumption that the waypoints are uniformly distributed in a given area $\mathcal{A}$. In some cases this may not be justified. In [12] a simulation-based approach is used to study the node distribution in the presence of a hot spot. In the model domain $\mathcal{A}$ is divided into two subdomains having waypoint intensities μ_1 and μ_2, with $\mu_1 > \mu_2$, so that $(A_1\mu_1 + A_2\mu_2)/(A_1 + A_2)$ (normalization). Domain 1 is referred to as the "attraction area" or hot spot.

In general, we may consider the RWP model with an arbitrary waypoint distribution with pdf $g(\mathbf{r})$. A similar analysis as is done in Section III for the uniform waypoint distribution yields that the spatial node distribution of a non-uniform random waypoint process is given by

$$f(\mathbf{r}) = \frac{1}{\mathrm{E}[\ell]} \int\limits_0^{2\pi} d\phi \int\limits_{a(\phi)}^{a(\phi+\pi)} dr_2 \int\limits_0^{a(\phi)} dr_1 \, (r_1 + r_2) \cdot g(r_1, \phi) \cdot g(r_2, \phi + \pi), \quad (10)$$

where $a(\phi) = a(\mathbf{r}, \phi)$ is the distance to the boundary from point $\mathbf{r}$ in direction ϕ and $g(r_i, \phi)$ is the pdf of the waypoints at point $\mathbf{r} + r_i \cdot (\cos\phi, \ \sin\phi)$. Let $a_1 = a(\phi)$ and $a_2 = a(\phi+\pi)$. Then, Eq. (10) can be written as

$$f(\mathbf{r}) = \frac{1}{\mathrm{E}[\ell]} \int\limits_0^{2\pi} d\phi \left[\int\limits_0^{a_1} dr_1 \, r_1 \cdot g(r_1, \phi) \cdot \int\limits_0^{a_2} dr_2 \, g(r_2, \phi + \pi) + \int\limits_0^{a_1} dr_1 \, g(r_1, \phi) \cdot \int\limits_0^{a_2} dr_2 \, r_2 \cdot g(r_2, \phi + \pi) \right],$$

which, due to symmetry, is equal to

$$f(\mathbf{r}) = \frac{2}{\mathrm{E}[\ell]} \cdot \int\limits_0^{2\pi} d\phi \left[\int\limits_0^{a_1} dr_1 \, r_1 \cdot g(r_1, \phi) \cdot \int\limits_0^{a_2} dr_2 \, g(r_2, \phi + \pi) \right]. \quad (11)$$
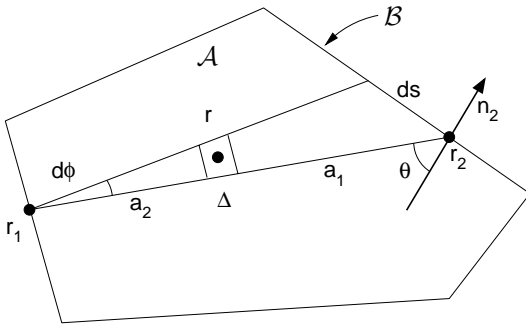
Fig. 10. Notation for analysis of RWPB.

Note that for the uniform waypoint distribution $g(r, \phi) = 1/A$ the general form (11) reduces to (3).

Similarly as in the case of a uniform waypoint distribution, the mean leg length can be obtained by normalisation,

$$
\begin{aligned}
\mathrm{E}[\ell] = 2 \int_{\mathcal{A}} dA \int_0^{2\pi} d\phi \cdot \\
\left[\int_0^{a_1} dr_1 \, r_1 \cdot g(r_1, \phi) \times \int_0^{a_2} dr_2 \, g(r_2, \phi + \pi) \right].
\end{aligned}
\tag{12}
$$

B. Random waypoint on border

Let us next consider a special case of RWP with arbitrary waypoints, i.e., the random waypoint on border (RWPB) model introduced in [12], where the destination points are chosen uniformly on the border $\mathcal{B}$ of the area. This model leads to a fundamentally different stationary node distribution than the RWP model, as will be shown later.

The stationary node distribution for the RWPB model can be derived by starting from the results of the non-uniform RWP model. Choosing the waypoint distribution as zero in points which are further than ϵ from the perimeter and some appropriate constant C_ϵ near the perimeter and letting $\epsilon \to 0$ one obtains the RWPB model and the respective stationary node distribution.

However, also in this case, it is possible to perform a similar analysis as in Section III for the traditional RWP model. This is probably more illustrative and we have chosen this approach. First the case of a general convex area is treated and then we consider two special cases, namely unit disk and unit square.

Curvilinear border: Consider first the case where the area $\mathcal{A}$ is convex and the curvature of the perimeter is positive everywhere. Hence, the perimeter does not contain any straight line segments and the probability of finding a node on the border is zero. To derive an expression for the node location distribution in this case, the initial steps in the analysis for the general convex area are basically the same as in the previous section for the standard RWP model, only the integrals are not over an area $\mathcal{A}$ but over a curve $\mathcal{B}$ with the length of the curve denoted by B. Now refer to Fig. 10, where $\mathbf{r}_1$ and $\mathbf{r}_2$ are two waypoints on the border. In the figure $dA = a_2 \cdot d\phi \cdot \Delta$ and $\mathbf{n}_2$ denotes the unit normal vector at $\mathbf{r}_2$. To compute the conditional expectation $\mathrm{E}[\ell \cap dA \,|\, P_1 = \mathbf{r}_1]$, it can be seen that

the integral equals Δ times the length of the line segment ds along the edge. Using the notation of the figure we obtain

$$
\begin{aligned}
\mathrm{E}[\ell \cap dA \,|\, P_1 = \mathbf{r}_1] &= \frac{1}{B} \Delta \, ds_2 = \frac{\Delta}{B} \frac{(a_1 + a_2) \cdot d\phi}{\cos\theta} \\
&= \frac{1}{B} dA \cdot \frac{a_1 + a_2}{a_2} \cdot \frac{1}{\cos\theta}.
\end{aligned}
$$

Similarly, as in the case of the RWP process, the above yields

$$
f_0(\mathbf{r}) = \frac{1}{\mathrm{E}[\ell]} \cdot \frac{\mathrm{E}[\ell \cap dA]}{dA} = \frac{1}{\mathrm{E}[\ell] B^2} \int_{\mathcal{B}} \frac{a_1 + a_2}{a_2 \cos\theta} \, ds, \tag{13}
$$

where $a_1 = |\mathbf{r} - \mathbf{r}_2|$, $a_2 = |\mathbf{r} - \mathbf{r}_1|$ and $\cos\theta = \mathbf{n}_2 \cdot (\mathbf{r}_2 - \mathbf{r}_1)/|\mathbf{r}_2 - \mathbf{r}_1|$ with $\mathbf{r}_1 = \mathbf{r}_1(s)$ and $\mathbf{r}_2 = \mathbf{r}_2(\mathbf{r}_1, \mathbf{r})$. For a given $\mathbf{r}$, let $\mathbf{a}_1 = \mathbf{a}_1(s) = \mathbf{r} - \mathbf{r}_2$ and $\mathbf{a}_2 = \mathbf{a}_2(s) = \mathbf{r} - \mathbf{r}_1$. With these, (13) can be written in a symmetric form,

$$
\begin{aligned}
f_0(\mathbf{r}) &= \frac{1}{\mathrm{E}[\ell] B^2} \int_0^B \frac{|\mathbf{a}_2 - \mathbf{a}_1|}{\mathbf{a}_2 \cdot \mathbf{n}_2} \, ds \\
&= \frac{1/2}{\mathrm{E}[\ell] B^2} \int_0^B |\mathbf{a}_2 - \mathbf{a}_1| \cdot \left(\frac{1}{\mathbf{a}_1 \cdot \mathbf{n}_1} + \frac{1}{\mathbf{a}_2 \cdot \mathbf{n}_2} \right) ds, \tag{14}
\end{aligned}
$$

where $\mathbf{n}_1 = \mathbf{n}_1(s)$ denotes the normal vector of the border at $\mathbf{r}_1(s)$.

General border: Now let us return to the question of an area $\mathcal{A}$, the perimeter of which may contain straight line segments. Assume that there are k line segments on the border $\mathcal{B}$ with lengths B_i, $i = 1, \ldots, k$, while the total length of the border is B. There is clearly a strictly positive probability that two consecutive waypoints reside on the same line segment and, consequently, that the node is on the border, i.e., $\mathbf{R} \in \mathcal{B}$. Thus, the system can be seen to be in two alternating states: "border mode" and "interior mode". The border mode corresponds to legs along some straight line segment and the interior mode corresponds to legs passing through the area. In particular, let p_i denote the probability that an arbitrary leg occurs on line segment i,

$$
\begin{aligned}
p_i &= \mathrm{P}\{\text{two consecutive waypoints on line segment } i\} \\
&= \left(\frac{B_i}{B} \right)^2,
\end{aligned}
$$

and p_0 the probability that a transition belongs to interior mode, for which we have

$$
p_0 = 1 - \sum_{i=1}^k p_i.
$$

As the arriving point and the departing point on any line segment i are uniformly distributed, the two modes (interior/border) can be treated separately. Thus, point $\mathbf{R}$ has a one-dimensional pdf on each line segment on the border $\mathcal{B}$, which are simply weighted versions of the one-dimensional RWP model pdf. However, in the interior mode the probability density of the nodes still obeys (13).

The one-dimensional RWP model has been studied in [12] and [13]. The results therein show that given that a node lies on a line segment $(0, L)$, its pdf is given by

$$
f(x) = \frac{6x(L - x)}{L^3}. \tag{15}
$$

Determination of the weights for modes: The appropriate weights for the interior mode and the border modes are equal to the respective time proportions. Let π_0 denote the proportion of time the node spends in the interior mode and π_i, $i = 1, \ldots, k$, the proportion of time it spends on line segment i. For the π_i we have the obvious relation,

$$\pi_j = \frac{p_j \mathrm{E}[\ell_j]}{\sum_{i=0}^k p_i \mathrm{E}[\ell_i]}, \tag{16}$$

where the $\mathrm{E}[\ell_i]$, $i = 1, \ldots, k$, correspond to the mean leg length on segment i, and $\mathrm{E}[\ell_0]$ corresponds to the mean leg length in the interior mode. The mean leg length of the whole process $\mathrm{E}[\ell]$ is the weighted sum,

$$\mathrm{E}[\ell] = p_0 \mathrm{E}[\ell_0] + p_1 \mathrm{E}[\ell_1] + \ldots + p_k \mathrm{E}[\ell_k]. \tag{17}$$

The mean leg length on line segment i is $\mathrm{E}[\ell_i] = B_i/3$ (see, e.g., [12] and [13]), and thus

$$\pi_0 = \frac{p_0 \mathrm{E}[\ell_0]}{\mathrm{E}[\ell]} = \frac{p_0 \mathrm{E}[\ell_0]}{p_0 \mathrm{E}[\ell_0] + \sum_{i=1}^k p_i B_i/3}. \tag{18}$$

In order to complete the analysis one still needs to determine the mean transition length in the interior mode, $\mathrm{E}[\ell_0]$, which can be achieved by a straightforward integration. Alternatively, integral of (13) over $\mathcal{A}$ is equal to π_0, which together with (18) allows us to determine $\mathrm{E}[\ell_0]$ and then $\mathrm{E}[\ell]$ by (17).

In summary, the RWPB node distribution can be characterized as follows. With probability π_0 the node lies in the interior of $\mathcal{A}$ having a conditional two-dimensional density given by (13), and with probability π_i the node is on the border line segment i, $i = 1, \ldots, k$, having a conditional one-dimensional density given by (15) with $L = B_i$,

$$\begin{cases} f_0(\mathbf{r}) = \pi_0 \cdot \dfrac{1}{p_0 \mathrm{E}[\ell_0] B^2} \displaystyle\int_{\mathcal{B}} \dfrac{a_1 + a_2}{a_2 \cos\theta} \, ds, \\[2mm] f_i(x) = \pi_i \cdot 6x(B_i - x)/B_i^3, \quad i = 1, \ldots, k. \end{cases} \tag{19}$$

C. Example: unit square

Consider next a unit square in which a node moves according to the RWPB model. Due to the symmetry we can concentrate on the x-axis first. The mean transition length in the interior mode, $\mathrm{E}[\ell_0]$, can be obtained from (19) by integration over the area. However, in this case $\mathrm{E}[\ell_0]$ can be obtained by a straightforward integration,

$$\begin{aligned} \mathrm{E}[\ell_0] &= \frac{2}{3} \int_0^1 \int_0^1 \sqrt{x^2 + y^2} \, dx \, dy \\ &\quad + \frac{1}{3} \int_0^1 \int_0^1 \sqrt{(x-y)^2 + 1} \, dx \, dy \\ &= \frac{1}{9}\left(2 + \sqrt{2} + 5\ln(1 + \sqrt{2})\right) \approx 0.869, \end{aligned}$$

and

$$\begin{aligned} \mathrm{E}[\ell] &= (3/4)\mathrm{E}[\ell_0] + (1/4) \cdot (1/3) \\ &= (1/12) \cdot \left(3 + \sqrt{2} + 5\ln(1 + \sqrt{2})\right) \approx 0.735. \end{aligned}$$
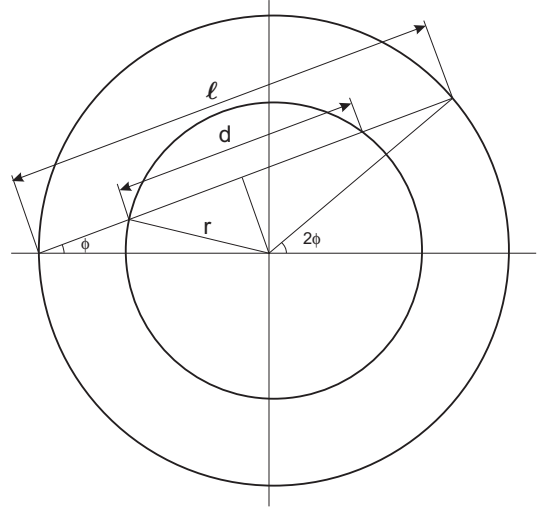
Fig. 12.   Notation for analysis of RWPB in a unit circle.

Thus, the proportion of time the node spends in the interior mode is

$$\pi_0 = \frac{2 + \sqrt{2} + 5\ln(1 + \sqrt{2})}{3 + \sqrt{2} + 5\ln(1 + \sqrt{2})} \approx 0.887,$$

and similarly, the proportion of time spent on each border line segment is,

$$\pi_i = \frac{1/4}{3 + \sqrt{2} + 5\ln(1 + \sqrt{2})} \approx 0.0283, \qquad i = 1, \ldots, 4.$$

Substituting the above in (19) gives the one-dimensional pdf on each border line segment,

$$f_i(x) = \pi_i \cdot 6x(1 - x) = \frac{3x(1 - x)}{6 + 2\sqrt{2} + 10\ln(1 + \sqrt{2})},$$

where $i = 1, \ldots, 4$. The two-dimensional pdf corresponding to interior points can be obtained by evaluating (19), as illustrated in Fig. 11.

D. Example: unit circle

In Section IV-B we have derived a general result (13) for the distribution of a node inside a given area when the waypoints are evenly distributed on the perimeter. Here we generalize the model a bit and derive the result in a more direct way for the unit circle. Instead of assuming that the next waypoint is chosen uniformly on the perimeter, we assume that the direction of the leg from the present waypoint to the next, defined by the angle ϕ between the radius to the current waypoint and the leg (see Fig. 12), also called the "bouncing angle", is randomly drawn from a distribution with a given pdf $f_\phi(\phi)$. For clarity, we assume that pdf of the bouncing angle is an even function, $f_\phi(\phi) = f_\phi(-\phi)$. It is easy to see that the uniform distribution $\phi \sim U(-\pi/2, \pi/2)$ corresponds to a uniform distribution of the waypoint on the perimeter.

We wish to calculate the radial distribution, $F_R(r)$, of the distance $R = |\mathbf{R}|$,

$$F_R(r) = \mathrm{P}\{|\mathbf{R}| \le r\}.$$
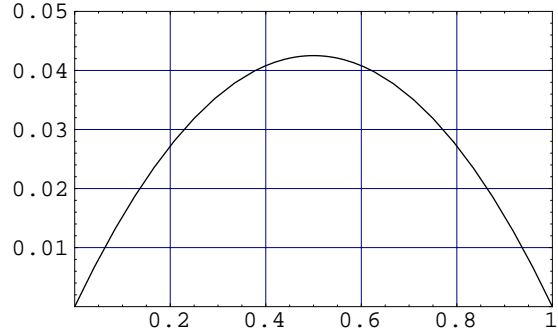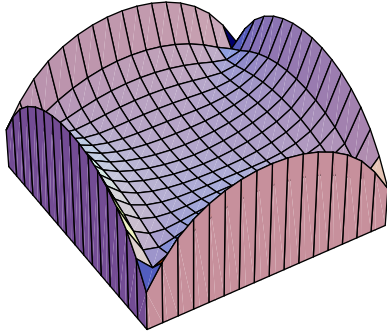
Fig. 11.   The pdf resulting from the RWPB model in unit square. The left figure corresponds to pdf of the interior mode, $f_0(\mathbf{r})$, and the right figure corresponds to pdf of the border mode, $f_i(r)$.

To this end, let $\ell(\phi)$ be the length of a random leg and $d(r,\phi)$ the length of the segment of $\ell(\phi)$ inside the circle of radius r, see Fig. 12. Both $\ell(\phi)$ and $d(r,\phi)$ are functions of the random variable ϕ. The required probability $F_R(r)$ is now given by $\bar{d}(r)/\mathrm{E}[\ell]$, where $\bar{d}(r) = \mathrm{E}[d(r,\phi)]$ and $\mathrm{E}[\ell] = \mathrm{E}[\ell(\phi)]$,

For a given ϕ we have from Fig. 12,

$$\begin{cases} d(r,\phi) & = \ 2\sqrt{r^2 - \sin^2\phi}, \\ \ell(\phi) & = \ 2\sqrt{1 - \sin^2\phi} \ \ = \ 2\cos\phi. \end{cases}$$

Denote by ϕ_0 the angle at which $d(r,\phi) = 0$,

$$\phi_0(r) = \arcsin r.$$

With the pdf $f_\phi(\phi)$ we then have the expected values,

$$\begin{cases} \bar{d}(r) & = \ 2\displaystyle\int_0^{\phi_0} d(r,\phi)f_\phi(\phi)\,d\phi, \\ \mathrm{E}[\ell] & = \ 2\displaystyle\int_0^{\pi/2} \ell(\phi)f_\phi(\phi)\,d\phi, \end{cases}$$

which lead to the result

$$F_R(r) = \frac{\bar{d}(r)}{\mathrm{E}[\ell]} = \frac{\displaystyle\int_0^{\phi_0}\sqrt{r^2 - \sin^2\phi}\,f_\phi(\phi)\,d\phi}{\displaystyle\int_0^{\pi/2}\sqrt{1 - \sin^2\phi}\,f_\phi(\phi)\,d\phi}.$$

For the uniform distribution, $f_\phi(\phi) = 1/\pi$ for $\phi \in (-\pi/2, \pi/2)$ and 0 otherwise, the expressions simplify:

$$\mathrm{E}[\ell] = \frac{2}{\pi}\int_0^{\pi/2} 2\cos\phi\,d\phi = \frac{4}{\pi}$$

in accordance with [17], and

$$F_R(r) = \int_0^{\phi_0}\sqrt{r^2 - \sin^2\phi}\,d\phi, \qquad (20)$$

which is an elliptic integral of the second kind.

The RWPB model with a uniform angle distribution in a unit disk is illustrated in Fig. 13, where the left graph shows the cumulative distribution function (cdf) $F_R(r)$ of the distance from the center, and the center and right graphs show the probability density function of the node's location at distance r in any direction, $f(\mathbf{r}) = f(r) = F'_R(r)/2\pi r$. From the center (and right) figure it can be seen that the density increases towards the perimeter. Recall that for the ordinary RWP model the density decreases to zero towards the border (cf. Fig. 5). This suggests that it should be possible to devise a RWP model with a non-uniform distribution of waypoints $\mathbf{X}$, which leads to a uniform distribution of the node location $\mathbf{R}$.

V. Applications

A. Connectivity in ad hoc networks

Connectivity properties are an essential reliability performance characteristic of ad hoc networks because of the use of multi-hop paths for communication. As part of earlier work in [21], we studied a network consisting of n nodes moving according to RWP within the unit circle and we have derived a very accurate approximation for the probability that the network is k-connected, i.e., that there are at least k node disjoint paths in the network. Here we apply Approximation 1 from [21] to compare the connectivity properties of RWP and RWPB, which have very different spatial properties.

Below we restate the approach used in [21] for the special case of 1-connectivity (i.e., probability that all nodes can reach all other nodes), since we will only concentrate on that. We consider n nodes moving within the unit disk. To define when two nodes are directly connected it is assumed that the coverage area of each node is circular with a radius of d and is denoted by $B_d(\mathbf{r})$, and that two nodes can hear each other's transmissions if they are within a distance of d from each other (i.e., we assume the so-called Boolean network model). Also, we denote by $p(r,d)$ the probability that a given node is within $B_d(\mathbf{r})$, where we emphasize that this probability depends only on the distance $r = |\mathbf{r}|$ from the center. We can express $p(r,d)$ as

$$p(r,d) = \int_{\mathbf{x}\in B_d(\mathbf{r})} f(|\mathbf{x}|)\,dA,$$
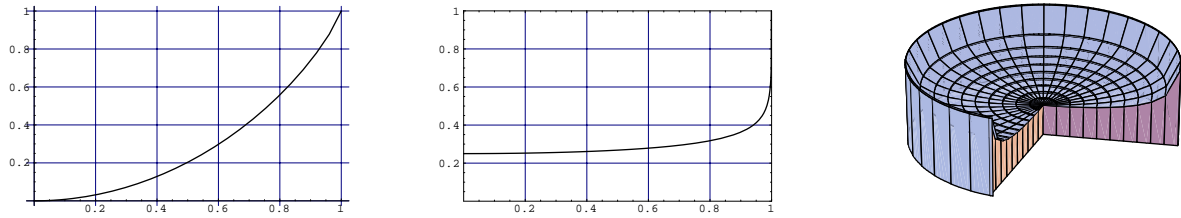
Fig. 13. The cdf $F_R(r)$ of the distance of the node from the origin (left) and the pdf $f(\mathbf{r}) = f(|\mathbf{r}|)$ of the node location (middle and right) for the RWPB model in a unit disk.

where $\mathbf{x}$ denotes the vector for the location of a point inside $B_d(\mathbf{r})$, and $f(\cdot)$ is the density of the RWP or RWPB process in a unit disk. The approximation is based on computing the probability that a given node has at least one neighbor, $Q_n(d)$. Since all nodes are independent and the probability that a node is at a distance r from the center equals $2\pi r f(r)$, $Q_n(d)$ is given by

$$Q_n(d) = 2\pi \int\limits_0^1 r f(r) \left(1 - (1 - p(r, d))^{n-1}\right) \, dr,$$

which is an exact result. Motivated by results in [23], we approximate 1-connectivity by

$$
\begin{aligned}
C_n(d) &= \mathrm{P}\{n\text{-node network is 1-connected}\} \\
&\approx (Q_n(d))^n .
\end{aligned}
\tag{21}
$$

Next we compare the impact of a uniform node location distribution, the RWP node location distribution, and the RWPB node location distribution on 1-connectivity. The results are shown in Fig. 14. The graphs show the probability of the network being 1-connected as a function of the transmission range d of each node for networks with $n = 20$ (left figure), $n = 100$, (middle figure), and $n = 500$ nodes (right figure). In each figure, the result for the RWP model is shown with dashed lines, the result for the RWPB model is shown with solid lines and the result for the uniform distribution is shown with dotted lines. To evaluate (21), for RWP $f(r)$ is given by (7), for RWPB $f(r) = F'(r)/(2\pi r)$ with $F(r)$ given by (20), and for the uniform distribution $f(r) = 1/\pi$.

As can be seen from the figure, for a small number of nodes the connectivity properties are better for RWP than RWPB or the uniform distribution. As the number of nodes is increased, the situation changes and RWPB and the uniform distribution yield better connectivity characteristics. Also note that the results for RWPB and the uniform distribution are close to each other, which is understandable as the RWPB node distribution is indeed quite close to uniform except near the border, see Fig. 13 (right).

It is worth noting that the minimum transmission range required to achieve a high connectivity probability increases slower with the RWP model than with the other two cases, i.e., adding one additional node has a smaller effect to connectivity with the RWP model than with the other two. This behavior is due to the different stationary node distributions and can be explained as follows. Roughly speaking, with the uniform node distribution and the RWPB model, the nodes are evenly distributed and the disconnected node may be located

anywhere. Also, an additional node is equally likely to appear in the neighborhood of the disconnected node, thus resolving the disconnected state of the network. With the RWP model the nodes are concentrated near the center of the area and a disconnected node is likely to be near the border. At the same time an additional node is more likely to be located in the center of the area and thus contributes less to the connectivity than is the case with uniformly distributed nodes or the RWPB model.

B. Traffic load in dense ad hoc network

Our next example considers network load in an idealized ad hoc network. The aim is to determine the pdf for the location of an arbitrary packet. The obtained pdf can then be interpreted as the traffic load distribution in the network with an appropriate scaling. Our initial assumptions and steps are similar to the ones in Pham and Perreau's work in [24] where the primary motivation has been to compare single-path routing to multi-path routing. The comparison between single-path and multi-path approaches is further extended in [25]. Both [24] and [25] assume a uniform node distribution in a disk. Here our aim is to apply the RWP formuæ to give an estimate for the traffic load in an ad hoc network with single-path routing where the network nodes may not be uniformly distributed [26].

Let $\lambda(r)$ denote the traffic rate experienced by a node located r units away from the center of a unit disk. The expression derived in [24] states that

$$\lambda(r) = (\pi\delta - 1) \cdot \lambda + \left(\pi(1 - r^2)\delta^2\beta\right)/2 \cdot \lambda, \tag{22}$$

where δ is the node density, λ the mean pairwise transmission rate and β some small positive constant reflecting the fact that the routes are not straight lines [24]. The first term corresponds to the node's own traffic, as $\pi\delta$ is equal the average number of nodes in a unit disk. The second term corresponds to the relayed traffic, which will be also our focus here. Thus, according to (22) the volume of the relayed traffic is some constant times $(1 - r^2)$.

In our idealized model we mean by traffic load the amount of (relayed) traffic passing through a differential area element around the node's location. We assume that the number of nodes is large and hence a typical route a packet takes consists of several hops and is roughly a straight line segment [24]. Furthermore, we assume that the average time it takes for a packet to travel from one location to another is directly proportional to the distance between the locations. This approximation
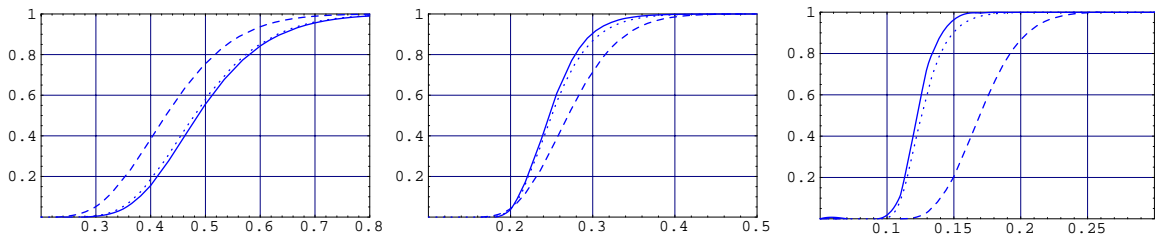
Fig. 14. Comparison of $C_n(d)$ with RWP node distribution (dashed lines), RWPB node distribution (solid lines), and uniform node distribution (dotted lines) for $n = 20, 100, 500$ nodes (from left to right).
.

is justified for straight line routes when the network load is low and queueing delays can be neglected. With these assumptions the process defining the location of a randomly chosen packet corresponds to the independent leg process (2) where the waypoints, i.e., the locations of the source and the destination node, are drawn from a given distribution. Hence, the stationary distribution of the packet location obeys the stationary node distribution of the corresponding non-uniform RWP process and can be obtained by evaluating (10) or (11).

Note that obtaining the mean number of packets residing in a given area is a matter of simple scaling. Consider a network with n nodes each with a (constant) transmission range of d. Let μ denote the mean transmission time of a packet and λ the average pairwise packet sending rate. Furthermore, let Λ denote the total sending rate of packets, $\Lambda = n(n-1)\lambda$. On average, the multi-hop route consists of $\mathrm{E}[\ell]/d$ hops and the packet transmission time at each hop is equal to $1/\mu$. Thus, for the mean sojourn time of a packet in the network we have $\bar{T} \approx \mathrm{E}[\ell]/(d \cdot \mu)$. By Little's result there are $\bar{N} = \Lambda \cdot \mathrm{E}[\ell]/(d \cdot \mu)$ packets under transmission on average. The mean number of packets in a given area is then obtained by multiplying the probability that a single packet moving according to the RWP model is in the area by $\bar{N}$.

As an example we consider two cases. In the first example, similarly as in [24], the nodes are assumed to be uniformly distributed in a unit disk. In the second example the nodes are assumed to be moving according to the (uniform) RWP process in a unit disk. When the nodes are uniformly distributed in a unit disk the stationary distribution of the location of the packet is clearly the same as the node distribution in the (uniform) RWP model, i.e., it is given by (7). Note that the polynomial approximation $P_1(r)$ of Table I for the node location in a unit disk is in fact equal to the relayed traffic term in (22) with an appropriate scaling.

Next, let us assume that the nodes move according to the (uniform) RWP process in a unit disk. Consequently, their stationary distribution is given by (7). Without loss of generality we can consider point $(0, h)$, for which the distance to the border in direction ϕ is given by

$$a(h, \phi) = \sqrt{1 - h^2 \cos^2 \phi} - h \sin \phi.$$

The waypoint distribution, resulting from the underlying uniform RWP process, depends only on the distance from the center of the disk, i.e., with a slight abuse of notation, we have $g(\mathbf{r}) = g(r)$ with $r = |\mathbf{r}|$. It turns out that if the waypoint distribution is a function of r^2 the integrand in (11) (or (10))

simplifies considerably. In particular, in this case (11) can be written as

$$f(h) = \frac{2}{\mathrm{E}[\ell]} \int\limits_0^{2\pi} d\phi \left[\int\limits_0^{a_1} dr_1 \, r_1 \cdot g^*(h^2 + r_1^2 + 2hr_1 \sin \phi) \cdot \right.$$
$$\left. \int\limits_0^{a_2} dr_2 \, g^*(h^2 + r_2^2 - 2hr_2 \sin \phi) \right],$$

where $g^*(r^2) = g(r)$, $a_1 = a(h, \phi)$ and $a_2 = a(h, \phi + \pi)$. Substituting to the above expression any polynomial approximation $P(r)$ with non-zero coefficients for the even degree terms yields an integral expression that can be easily evaluated.

Here we have chosen to use $P_2(r)$ from Table I, for which the normalization condition gives the mean leg length, $\mathrm{E}[\ell] \approx 0.715$. For the uniform waypoint distribution the mean leg length in a unit disk is considerably higher, $\mathrm{E}[\ell] \approx 0.905$. Note that the mean leg length corresponds to the mean route length in our ad hoc network model. The resulting pdf's are illustrated in Fig. 15. On the left figure the (initially) lower curve corresponds to the packet distribution with a uniform network node distribution, and the upper curve corresponds to the packet distribution when the network nodes move according to the (uniform) RWP mobility model. From the figure it can be seen that with the RWP mobility model probability mass gets more concentrated around the center of the area than in the case of uniform node distribution. Hence, as intuition suggests, the relayed traffic load with nodes moving according to the (uniform) RWP model is considerably higher in the center of the area than is the case with uniformly distributed nodes.

VI. CONCLUSIONS

One of the most widely used mobility models is the RWP model. We have analyzed the spatial distribution of a node moving according to the RWP model. The main result of our paper is the general expression giving the node distribution up to a normalization constant. While the approach shares some similarities with the work in [13], we directly consider an arbitrary convex domain and are able to perform the derivations without any approximations. The resulting expression consists of a one-dimensional integral, which is easy to evaluate numerically for any given geometry. The results have been illustrated for several geometries (unit circle, unit square, and hexagon) for which also accurate polynomial approximations have been given. In general the shape of the node distribution for any geometry is such that the probability mass is concentrated
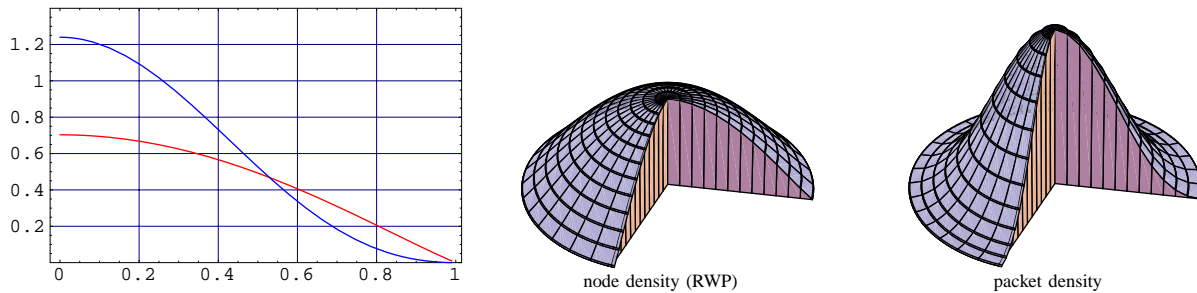
Fig. 15. On the left figure the lower curve corresponds to the pdf of the node location according to RWP model, and the upper curve the pdf of the packet location in a dense ad hoc network. The figures on the right illustrate the respective pdfs in 3-dimensions.

in the center of the area, where the equivalue contours are circular/elliptical, and the density decreases roughly linearly towards the borders with the equivalue contours gradually transforming to curves resembling the geometry of the considered area.

We have also provided results on a generalization of the basic RWP model where the locations of the waypoints are drawn from an arbitrary distribution. As a special case we have analyzed the RWPB model, where the waypoints are located on the border of the area. If the border contains straight line segments, the distribution of the location of the node is composed of two components corresponding to the border mode and the interior mode. We have given general expressions for both components of the node distribution. An explicit result was derived for the unit circle, having only the interior component. In general, the node distribution in the RWPB model differs from the RWP model by concentrating the probability mass near the border of the area and, eventually, yielding a non-zero probability mass on the border if it contains straight line segments.

In addition to the application to efficient sample generation, our results can also be applied to study certain performance quantities in a wireless multihop network with mobile users. In this paper, we have given two such applications. As a first application, we have considered connectivity properties of an ad hoc network with nodes moving according to different patterns The connectivity of the network has been studied, e.g., in [21] and [22] where it is assumed that the nodes are either uniformly distributed or move according to (basic) RWP process. The performance quantity of interest has been the probability that a network is (1-)connected, for which accurate approximations have been given. In this paper we have used the same approach to evaluate the difference between the RWP model, RWPB model and the assumption that nodes are uniformly distributed in the region. The comparison showed that the connectivity properties of RWP and RWPB yield very different results; connectivity properties under RWP are better than with RWPB or the uniform distribution when the number of nodes is small, and vice versa for a large number of nodes.

As a second application, the results were used to quantify and we were able to analyze the traffic load in a dense ad hoc network. Under certain assumptions we are able to derive an expression for the network load in an ad hoc network with an arbitrary node distribution. As an example we have studied the traffic load with the node distribution resulting from the RWP model and compared it with the load resulting from the uniform node distribution. The result has been obtained by using the integral expression for spatial node distribution of non-uniform RWP model together with a polynomial approximation for the node pdf according to the uniform RWP model. The results show that due to the mobility the traffic load increases even more in the center of the area than in the case of uniformly located nodes.

Regarding future work, the RWP mobility model itself perhaps offers limited scope for further extensions and new useful analytical results. However, some of the methods developed in this work may be found useful also in the analysis of more elaborate and realistic mobility models.

ACKNOWLEDGMENT

REFERENCES

[1] David B Johnson and David A Maltz, "Dynamic source routing in ad hoc wireless networks," in *Mobile Computing*, Imielinski and Korth, Eds., vol. 353. Kluwer Academic Publishers, 1996.

[2] M. Grossglauser and D. N. C. Tse, "Mobility increases the capacity of ad hoc wireless networks," *IEEE/ACM Transactions on Networking*, vol. 10, no. 4, August 2002.

[3] P. Gupta and P. R. Kumar, "The capacity of wireless networks," *IEEE Transactions on Information Theory*, vol. 46, no. 2, March 2000.

[4] O. Dousse, P. Thiran, and M. Hasler, "Connectivity in ad-hoc and hybrid networks," in *Proceedings of IEEE INFOCOM*, New York, June 2002.

[5] M. D. Penrose, "On k-connectivity for a geometric random graph," *Random Structures and Algorithms*, vol. 15, no. 2, pp. 145–164, 1999.

[6] Peng-Jun Wan and Chih-Wei Yi, "Asymptotic critical transmission radius and critical neighbor number for k-connectivity in wireless ad hoc networks," in *Proceedings of ACM MobiHoc '04*. 2004, pp. 1–8, ACM Press.

[7] J. Yoon, M. Liu, and B. Noble, "Random waypoint considered harmful," in *Proceedings of IEEE INFOCOM*, San Fransisco, California, USA, April 2003, pp. 1312–1321.

[8] W. Navidi and T. Camp, "Stationary distributions for the random waypoint mobility model," *IEEE Transactions on Mobile Computing*, vol. 3, no. 1, pp. 99–108, January-March 2004.

[9] C. Bettstetter, H. Hartenstein, and X. Pérez-Costa, "Stochastic properties of the random waypoint mobility model," *ACM/Kluwer Wireless Networks: Special Issue on Modeling and Analysis of Mobile Networks*, vol. 10, no. 5, Sept. 2004.

[10] J. Le Boudec and M. Vojnović, "Perfect simulation and stationarity of a class of mobility models," in *Proceedings of IEEE INFOCOM '05*, 2005, pp. 2743–2754.

[11] Jungkeun Yoon, Mingyan Liu, and Brian Noble, "Sound mobility models," in *MobiCom '03: Proceedings of the 9th annual international conference on Mobile computing and networking*, New York, NY, USA, 2003, pp. 205–216, ACM Press.

[12] C. Bettstetter and C. Wagner, "The spatial node distribution of the random waypoint mobility model," in *Proceedings of German Workshop on Mobile Ad Hoc networks (WMAN)*, Ulm, Germany, March 2002.

[13] C. Bettstetter, G. Resta, and P. Santi, "The node distribution of the random waypoint mobility model for wireless ad hoc networks," *IEEE Transactions on Mobile Computing*, vol. 2, no. 1, pp. 25–39, 2003.

[14] Esa Hyytiä, Pasi Lassila, Laura Nieminen, and Jorma Virtamo, "Spatial node distribution in the random waypoint mobility model," Tech. Rep. TD(04)029, COST279, Sept. 2004.

[15] Esa Hyytiä and Jorma Virtamo, "Random waypoint model in n-dimensional space," *Operations Research Letters*, vol. 33/6, pp. 567–571, Nov. 2005.

[16] Eric W. Weisstein, "Disk line picking," From MathWorld – A Wolfram Web Resource.

[17] Eric W. Weisstein, "Circle line picking," From MathWorld – A Wolfram Web Resource.

[18] Eric W. Weisstein, "Square line picking," From MathWorld – A Wolfram Web Resource.

[19] J. Le Boudec, "On the stationary distribution of speed and location of random waypoint," *IEEE Transactions on Mobile Computing*, Dec. 2005.

[20] D. Stoyan, W. S. Kendall, and J. Mecke, *Stochastic geometry and its applications*, Wiley, Chichester, England, second edition, 1995.

[21] P. Lassila, E. Hyytiä, and H. Koskinen, "Connectivity properties of random waypoint mobility model for ad hoc networks," in *The Fourth annual Mediterranean workshop on Ad Hoc Networks (Med-Hoc-Net 2005)*, Île de Porquerolles, France, June 2005.

[22] Christian Bettstetter, "On the connectivity of Ad Hoc networks," *Computer Journal*, vol. 47, no. 4, pp. 432–447, July 2004.

[23] M. D. Penrose, "Extremes for the minimal spanning tree on normally distributed points," *Advances in Applied Probability*, vol. 30, no. 3, pp. 628–639, 1998.

[24] P. P. Pham and S. Perrau, "Performance analysis of reactive shortest path and multi-path routing mechanism with load balance," in *Proceedings of IEEE INFOCOM*, San Fransisco, California, USA, April 2003, pp. 251 – 259.

[25] Y Ganjali and A. Keshavarzian, "Performance analysis of reactive shortest path and multi-path routing mechanism with load balance," in *Proceedings of IEEE INFOCOM*, Hong Kong, China, mar 2004, pp. 1120–1125.

[26] Esa Hyytiä, Pasi Lassila, Aleksi Penttinen, and János Roszik, "Traffic load in dense wireless multihop network," in *The 2nd ACM International Workshop on Performance Evaluation of Wireless Ad Hoc, Sensor, and Ubiquitous Networks (PE-WASUN 2005)*, Montreal, Quebec, Canada, Oct. 2005, pp. 9–17.

APPENDIX

A. Alternative expression for mean leg length in RWP with uniform waypoint distribution

Alternatively, we can calculate $E[\ell]$ directly based on its definition as the average distance between two points randomly located in the area $\mathcal{A}$,

$$E[\ell] = \frac{1}{A^2} \int_{\mathcal{A}} d^2\mathbf{r}_1 \int_{\mathcal{A}} d^2\mathbf{r}_2 \, |\mathbf{r}_2 - \mathbf{r}_1|.$$

Instead of $\mathbf{r}_2$ we use a new variable of integration, $\mathbf{r} = \mathbf{r}_2 - \mathbf{r}_1$,

$$E[\ell] = \frac{1}{A^2} \int d^2\mathbf{r}_1 \int d^2\mathbf{r} \, 1_{\mathbf{r}_1 \in \mathcal{A}} \, 1_{\mathbf{r}_1 + \mathbf{r} \in \mathcal{A}} \, r,$$

and define
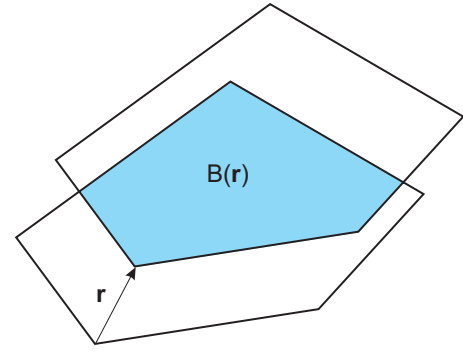
Fig. 16.   Illustration of the translation operation.
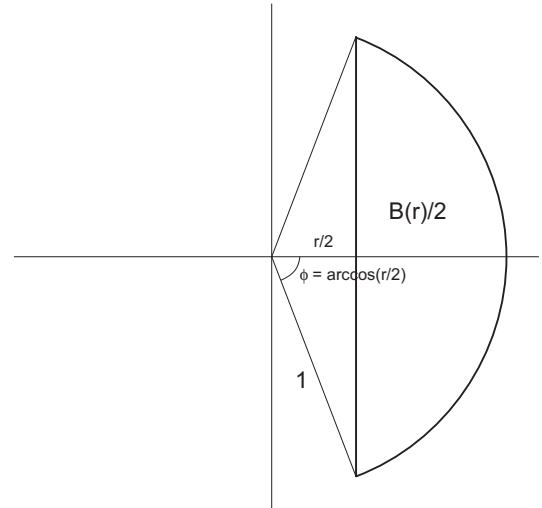
Fig. 17.   Illustration of the translation for unit disk.

$$B(\mathbf{r}) = \int d^2\mathbf{r}_1 \, 1_{\mathbf{r}_1 \in \mathcal{A}} \, 1_{\mathbf{r}_1 + \mathbf{r} \in \mathcal{A}} = \int d^2\mathbf{r}_1 \, 1_{\mathbf{r}_1 \in \mathcal{A} \cap (\mathcal{A} - \mathbf{r})}$$

as the area of the intersection of $\mathcal{A}$ and its copy translated by the vector $-\mathbf{r}$, yielding

$$E[\ell] = \frac{1}{A^2} \int d^2\mathbf{r} \, r B(\mathbf{r}) = \frac{1}{A^2} \int_0^D dr \int_0^{2\pi} d\phi \, r^2 B(r, \phi). \quad (23)$$

It is obvious that $B(\mathbf{r}) = B(-\mathbf{r})$ as the area of the intersection depends only on the relative positions. The translation operation and the function $B(\mathbf{r})$ are illustrated in Figure 16. The integration in (23) is formally over the whole plane. Note, however, that $B(\mathbf{r}) = B(r, \phi)$ is zero for any translation longer than the greatest diameter D of the area $\mathcal{A}$. The new expression (23) for $E[\ell]$ is equivalent to (5), though this is not apparent by just looking at the expressions.

Unit disk: In this case the area of the intersection $B(\mathbf{r})$ does not depend on the direction of the translation but is just a function of r, the length of the translation, $B(\mathbf{r}) = B(r)$, and equals twice the area of the segment of a unit disk as shown in Figure 17. Thus we have

$$E[\ell] = \frac{2\pi}{A^2} \int_0^2 dr \, r^2 B(r),$$

where

$$B(r) = 2 \arccos\left(\frac{r}{2}\right) - r\sqrt{1 - \left(\frac{r}{2}\right)^2}.$$

The integral can again be evaluated explicitly and we obtain

$$\mathrm{E}[\ell] = \frac{128}{45\pi} \approx 0.905,$$

in accordance with (8).

Rectangular Area: In the case of a rectangular area with a and b denoting the lengths of the sides, we have $B(r, \phi) = (a - r\cos\phi)^+(b - r\cos\phi)^+$. Due to symmetry it is sufficient to consider $\phi \in [0, \pi/2]$. We change the order of integration in (23) and eliminate the +-operator in $B(r, \phi)$ by introducing the function $g(\phi)$ which gives the proper integration range for r up to which the areas of the rectangles still overlap in a given direction ϕ,

$$g(\phi) = \begin{cases} \frac{a}{\cos\phi}, & 0 \le \phi < \arctan\frac{b}{a}, \\ \frac{b}{\sin\phi}, & \arctan\frac{b}{a} \le \phi < \frac{\pi}{2}. \end{cases}$$

Hence, (23) can be expressed as

$$\mathrm{E}[\ell] = \frac{4}{a^2 b^2} \int_0^{2\pi} d\phi \int_0^{g(\phi)} r^2 (a - r\cos\phi)(b - r\cos\phi)\, dr$$

$$= \frac{1}{a^2 b^2} \int_0^{\pi/2} g(\phi)^3 \cdot \left(\frac{4}{3}ab - \right.$$

$$\left. g(\phi)(b\cos\phi + a\sin\phi) + \frac{2}{5}g(\phi)^2 \sin 2\phi \right) d\phi.$$

The above integral can be easily evaluated numerically. For example for a unit square with $a = b = 1$ the above yields $\mathrm{E}[\ell] = 0.521$ in accordance with results from [13].

Esa Hyytiä received the M.Sc. (Tech.) degree in engineering physics and D.Sc. (Tech.) degree in electrical engineering from the Helsinki University of Technology, in 1998 and 2004, respectively. He is currently working at the Centre for Quantifiable Quality of Service in Communication Systems, Centre of Excellence, Norwegian University of Science and Technology, Trondheim, Norway. His current research interests include performance analysis, design and optimization of wireless multihop and IP networks.

Pasi Lassila received the M.Sc. (Tech.) and D.Sc. (Tech.) degrees in electrical engineering from the Helsinki University of Technology in 1993 and 2001, respectively. He is currently working as a senior researcher in the Networking Laboratory at Helsinki University of Technology. His current research interests include performance evaluation of fixed IP-based data networks, such as TCP modeling and analysis, as well as performance analysis of multihop wireless ad hoc networks and mobility modelling.

Jorma Virtamo received the M.Sc. (Tech.) degree in engineering physics and D.Sc. (Tech.) degree in theoretical physics from the Helsinki University of Technology, in 1970 and 1976, respectively. In 1986, he joined the Technical Research Centre of Finland, VTT Information Technology, where he led a teletraffic research group, and became a Research Professor in 1995. Since 1997 he has been a Professor in the Networking Laboratory of the Helsinki University of Technology. His current research interests include queueing theory and performance analysis of the Internet, ad hoc networks and peer-to-peer networks.